



저작자표시-비영리-변경금지 2.0 대한민국

이용자는 아래의 조건을 따르는 경우에 한하여 자유롭게

- 이 저작물을 복제, 배포, 전송, 전시, 공연 및 방송할 수 있습니다.

다음과 같은 조건을 따라야 합니다:



저작자표시. 귀하는 원저작자를 표시하여야 합니다.



비영리. 귀하는 이 저작물을 영리 목적으로 이용할 수 없습니다.



변경금지. 귀하는 이 저작물을 개작, 변형 또는 가공할 수 없습니다.

- 귀하는, 이 저작물의 재이용이나 배포의 경우, 이 저작물에 적용된 이용허락조건을 명확하게 나타내어야 합니다.
- 저작권자로부터 별도의 허가를 받으면 이러한 조건들은 적용되지 않습니다.

저작권법에 따른 이용자의 권리는 위의 내용에 의하여 영향을 받지 않습니다.

이것은 [이용허락규약\(Legal Code\)](#)을 이해하기 쉽게 요약한 것입니다.

[Disclaimer](#)

Master's Thesis

Conversion of Polyacrylonitrile to Nitrogen-Doped Graphene

Han Jae Nam

Department of Energy Engineering
(Energy Engineering)

Graduate School of UNIST

2018

Conversion of Polyacrylonitrile to Nitrogen-Doped Graphene

Han Jae Nam

Department of Energy Engineering
(Energy Engineering)

Graduate School of UNIST

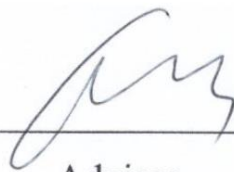
Conversion of Polyacrylonitrile to Nitrogen-Doped Graphene

A thesis/dissertation
submitted to the Graduate School of UNIST
in partial fulfillment of the
requirements for the degree of
Master of Science

Han Jae Nam

06. 05. 2018 Month/Day/Year of submission

Approved by



Advisor

Hyeon Suk Shin

Conversion of Polyacrylonitrile to Nitrogen-
Doped graphene

Han Jae Nam

This certifies that the thesis/dissertation of Han Jae Nam is approved.

06.05.2018 Month/Day/Year of submission



Advisor: Hyeon suk Shin



Hyesung Park



Soon-Yong Kwon

Abstract

Since graphene was obtained from graphite via a mechanical exfoliated method by Geim et al. in 2004, it has been regarded as a promising material because of its outstanding properties. In particular, nitrogen-doped graphene (N-doped graphene) is anticipated for industrial use because of the widening of the graphene bandgap, and the potential to offer a catalytic site to oxygen reduction reaction, ultra-capacitor, etc. Most N-doped graphene are synthesized using ammonia or hydrazine as precursor. However, these materials could be pose enormous hazards to people. Herein, we report conversion of polyacrylonitrile to N-doped graphene with nitrogen percentage up to 2%–4%. Polyacrylonitrile (PAN), which is a well-known precursor to carbon fiber, is an appropriate material for the commercialization of N-doped graphene because it is already produced by many companies. Because the linear formula of PAN is $(C_3H_3N)_n$, a nitrogen compound material is not required. PAN is spin-coated on Pt foil, which exhibits a catalytic effect to form graphene. The PAN/Pt foil was heated to 200°C for stabilization in air and 800°C–1000°C for graphitization with hydrogen gas. The stabilization process is an important factor to consider in order to obtain continuous N-doped graphene films. An atomic force microscope and scanning electron microscope confirmed that N-doped graphene forms continuous film with single layer. Raman spectroscopy demonstrated nitrogen doping induced D band and blueshift of G band. X-ray photoelectron spectroscopy showed that the atomic ratio of nitrogen in graphene was approximately 2%–3.5%; additionally, pyrrolic-N was dominant. The N-doped graphene filed effect transistors exhibit an n-type behavior.

Contents

Abstract.....	I
List of figures.....	III
1. Introduction: Research background for conversion of polyacrylonitrile to N-doped graphene	1
1.1 Properties of graphene	1
1.2 Properties of N-doped graphene.....	2
1.3 Synthesis methods of graphene.	2
1.3.1 Synthesis of graphene using polymers as precursor	6
1.3.2 Synthesis of N-doped graphene.....	6
1.4 Future of graphene	7
2. Conversion of polyacrylonitrile to N-doped graphene	8
2.1 Experimental section.....	8
2.1.1 Conversion of polyacrylonitrile to N-doped graphene using CVD.....	8
2.1.2 Transfer method	9
2.1.3 FET fabrication	9
2.1.4 Characterization	9
2.2 Result and discussion	11
2.3 Conclusion	22
REFERENCES	23

List of Figures

Figure 1. (a) Geometry of graphene. (b) Bonding of one carbon atom in graphene. (c) Band diagram of graphene at $K = 0$ point. ¹	5
Figure 2. Schematic of N-doped graphene.....	6
Figure 3. Examples of graphene application in various area. ²	7
Figure 4. (a) Molecular structure of PAN. (b) The stabilized PAN structure. ³ (c) Structure changes for PAN precursor during carbonization. ⁴	10
Figure 5. (a) Experiment process of conversion of PAN to N-doped graphene using CVD. (b) XPS C 1s spectrum of the PAN. (c) XPS C 1s spectrum of the stabilized PAN.	13
Figure 6. (a) SEM image of the N-doped graphene without stabilization process. (b) SEM image of the N-doped graphene growth at vacuum during the stabilization process.	14
Figure 7. (a) Optic image of the N-doped graphene. (b) SEM image of the N-doped graphene. (c) AFM image of the N-doped graphene. (d) The height profile which was taken from (c) the white line.....	15
Figure 8. Raman spectra of the N-doped graphene, the spectrum of red line is pristine graphene. The spectrum of the blue line is the N-doped graphene.....	16
Figure 9. (a) XPS spectrum of the N-doped graphene on $\text{SiO}_2(300 \text{ nm})/\text{Si}$ substrate. (b) XPS C 1s spectrum and (c) XPS N1s spectrum of the N-doped graphene on $\text{SiO}_2(300 \text{ nm})/\text{Si}$ substrate. The inset image exhibits XPS N1s spectrum of cleaned SiO_2/Si substrate. (d) Graph of Atomic N ratio.	17
Figure 10. (a) XPS N 1s spectra of N-doped graphene with temperature. (b) Graph of N-doped graphene nitrogen configuration with temperature.....	18
Figure 11. Optic image of different concentrations of PAN after the same conversion condition not using Pt but using Cu. (a) and (b) were used 0.5 and 5% PAN solution. (c). Raman spectra of PAN after the same conversion condition using Cu. Red and blue line were used 0.5 and 5% PAN solution.....	19
Figure 12. (a) Schematic of the N-doped graphene FET device. (b) Optic image of the N-doped graphene device. (c) I_{ds}/V_{ds} characteristics at various V_g for the N-doped graphene FET. Devices. (d) I_{ds}/V_g curve of the N-doped graphene ($V_{ds} = 1 \text{ V}$). the inset figure shows I_{ds}/V_{ds} characters without V_g	20

1. Introduction: Research background for conversion of polyacrylonitrile to N-doped graphene

Graphene is a single layer carbon film with honeycomb lattices. Since graphene was obtained from graphite using a “scotch tape” method by Geim et al. in 2004,⁵ various sorts of graphene have been regarded as the next generation materials because of their superior characteristics.

1.1 Properties of graphene

The structure of graphene is two-dimensional crystalline consisting of a single layer with honeycomb lattices. Graphene has two types of edges: an “armchair” edge and a “zig-zag” edge (figure 1a). Carbon atom has 2s, 2p_x, 2p_y, 2p_z atomic orbitals. In graphene, sp² orbital hybridization occurs by mixing 2s, 2p_x, and 2p_y. The sp² orbitals constitute three σ bonds with combination neighbor atoms. The remaining 2p_z orbital forms a π-bond. The π-bonds in graphene of carbon atoms hybridize together to produce a valence band filled with electrons and a conduction band which is empty (figure 1b). At K = 0 point, the valence band and the conduction band meet each other with linear dispersion, i.e., here, the graphene has no band gap (figure 1c).¹

Graphene electron mobility is $2.5 \times 10^5 \text{ cm}^2\text{V}^{-1}\text{s}^{-1}$ at room temperature.⁶ Additionally, graphene has noble electronic properties like quantum Hall effects,⁷ ballistic transports, and ambipolar electric field effects.³

Graphene shows not only superb electronic properties but also impressive mechanical properties. In 2008, Hone et al. measured the stiffness of free-standing graphene, using the tip of an atomic force microscope (AFM), and observed that it is not affected by the surrounding environment. They obtained the Young’s modulus of approximately 1.0 TPa and intrinsic tensile strength of 130.5 GPa. In their thesis, they noted that graphene was the strongest material among the materials measured.⁸ Later, JU Lee et al. obtained a more precise Young’s modulus value of approximately 2.4 TPa, which value is 120 times stronger than steel by Raman spectroscopy measurement.⁹ However, graphene’s fracture toughness is approximately $4 \text{ MPa}\sqrt{\text{m}}$. The value demonstrates that graphene is relatively brittle compared to its strength.

The opacity of monolayer graphene is widely known to be $\pi\alpha = 2.3 \%$ in the visible range,¹⁰ because theoretically, the thickness of monolayer graphene is approximately 0.345 nm.¹¹ The transmittance of graphene decreases as the number of graphene layers increases. Graphene on SiO₂/Si substrate exhibit an interference effect of light reflection.¹² Hence, Graphene on SiO₂/Si substrate can be observed with the naked eye. The refractive index of graphene was reported to be in the range $n = 2.0i - 1.1i$ ¹¹ as a

monolayer, and in the range $n = 2.6i-1.3i^{13}$ as bulk graphite in the visible range.

1.2 Properties of N-doped graphene

Graphene has been considered a promising material to replacing silicon because of its remarkable electronic properties. It is difficult to put to industrial use because of the absence of a bandgap, which is essential for semiconductor switching in pristine graphene. Doping is a well-known method for changing the semiconducting properties in industry. Boron and nitrogen are commonly used as doping atoms in carbon materials because their atom sizes are similar to the size of a carbon atom. Boron and nitrogen contain one additional hole and electron when these atoms substitute carbon atoms in graphene. Thus, boron and nitrogen act as hole acceptor and electron donor of carbon materials. As a result, doped graphene exhibits a change in its electronic structure, thereby widening its bandgap.¹⁴ There are three substitutional sites when nitrogen atom is doped into graphene (Figure 2).¹⁵ The first is pyridinic N, which is located at the defects or edges in graphene. Pyridinic N contributes a p electron to the π system. The second is graphitic N, which is located at the hexagonal ring by the substitution site of carbon. The third is pyrrolic N, which bonds with two carbon atoms in five-membered ring and gives two electrons to the π system. When nitrogen atoms substitute carbon atoms in graphene lattice, the nitrogen atoms prefer pyrrolic-N or pyridinic-N sites because of stable thermal energy.¹⁶

1.3 Synthesis methods of graphene.

Graphene synthesis methods have been developed to a scalable and high-quality level since the introduction of the exfoliated method. There are four main methods of obtaining graphene, which are, mechanical peeling method,⁵ chemical vapor deposition (CVD) using gas or solid precursors on catalyst substrates,¹⁷⁻¹⁸ reduction of graphene oxide,¹⁹ and epitaxial graphene growth using SiC substrates.²⁰ It is widely known that graphene synthesis method affects graphene quality and scale. For example, mechanical peeling methods produce high-quality graphene, however this technique has limitations in growing large areas and large amounts of graphene. In epitaxial graphene growth method, pyrolysis occurs on the SiC substrate to form graphene. However, this method has drawbacks in controlling thickness and cost. The growth of graphene using CVD is used in many laboratories and is a well-known growth method for obtaining graphene. Since Li et al. demonstrated that graphene can grow on Cu foil using methane gas, this method is commonly used in many laboratories to obtain high-quality

graphene because it produces graphene at an affordable price and in an easy way.²¹ Not only Cu, but also other metals such as Pt,²² Ni,²¹ Ru,²³ and Ge²⁴ are used as catalysts for graphene growth. Gao et al. showed repeatable graphene growth on Pt. Although, Pt is a more expensive material than Cu foil, growth on Pt has strong points, repeatable use, and small wrinkles owing to similar thermal coefficients between Pt and graphene.

1.3.1 Synthesis of graphene using polymers as a precursor

Graphene can be formed not only using gas but also solid carbon sources. In 2007, poly (methyl methacrylate), called PMMA, was converted to graphene on Cu substrates.¹⁸ Thereafter, many researchers have tried to find appropriate polymers that can be used to grow graphene. For example, Yan et al. demonstrated a direct growth of bilayer graphene by insulating substrates without transfer process using PMMA, Poly(2-phenylpropyl)methylsiloxane (PPMS), polystyrene (PS), and poly(acrylonitrile-co-butadiene-co-styrene) (ABS).²⁵ These polymers were converted to graphene under the Ni layer. Additionally, Byun et al. demonstrated direct graphene growth on SiO₂ substrate from PMMA, PAN, PS which are common polymers with evaporated Ni layer.²⁶

Choosing polymers as the precursor to graphene is an option toward the commercialization of graphene. First, polymers are relatively safer than hydrocarbon gases. Although, there are numerous studies on hydrocarbon gases as a graphene source, hydrocarbon gases have the possibility of explosion, which becomes an obstacle to mass production. Additionally, polymers are appropriate to industrialization of graphene because they are easily coated on substrates, such as spin-coating and Langmuir-Blodgett method. Finally, polymers are likely to be designed to synthesize graphene at low temperatures or to produce high-quality graphene. For example, Jo et al. reported growth of monolayer graphene without using the characterization of Benzophenone tetracarboxylic dianhydride-phenylenediamine properties.²⁷ Furthermore, Cho et al. reported the synthesis of graphene at low temperatures using poly aromatic hydrocarbons.²⁸

1.3.2 Synthesis of N-doped graphene

Recently, many scientists have reported N-doped graphene growth and its application.²⁹⁻³² There are two main methods for the synthesis of doped graphene: the first is growth in CVD method, and the second is post-synthesis treatment. In the CVD method, the nitrogen compounds are introduced during

the graphitization process. Luo, Z group showed that the nitrogen content of graphene could be modulated by nitrogen/methane flow rate.³³ However, this method dangerous because of its use of ammonia, which is hazardous to humans. Additionally, Panchokarla group reported the synthesis of boron and nitrogen doped graphene by an arc discharge method.³⁴ However, the arc discharge method has the possibility of damaging graphene. Post-synthesis treatment methods often require high temperatures. Qian liu et al. reported they converted graphene to N-doped graphene in ammonia gas at high temperatures.³⁵ Shao et al. reported N-doped graphene fabricated using graphene oxide with melamine at high temperatures.³⁶ However, this method has the limitation that graphene oxide is not suitable for high-quality materials because of its many impurities.

1.4 Future of graphene

Graphene is one of the promising materials that will vastly revolutionize industries because of its superb properties. In modern electronics, ITO is the most widely used material for the transparent anode in optoelectronics. However, ITO has several defects, such as poor flexibility, difficulty of etching, and high price. Graphene has the potential to replace ITO because of its excellent conductivity. In addition, because of excellent flexibility, it can be used for flexible electronics.³⁷ Additionally, it can be used in fuel cells. Graphene acts as a selective barrier that blocks hydrogen atoms and passes protons.³⁸

N-doped graphene has the potential to be commercialized in various sectors. For example, N-doped graphene could be used to increase the performance of lithium ion batteries because of the high surface area, flexibility, and high electrical electronic properties. Wang group reported N-doped graphene containing 2% nitrogen that showed 900 mAh/g reversible capacity at a current density of 42 mA.³⁹ Furthermore, Reddy et al. demonstrated that N-doped graphene has almost double the reversible discharge capacity of graphene because of Li ion intercalation occurring with nitrogen atoms.⁴⁰ N-doped graphene is one of the materials suitable for replacing Pt with respect to oxygen reduction reaction (ORR). Nitrogen atoms in graphene change the atomic charge distribution. Additionally, N-doped graphene usually exhibits a high spin density. Kurak et al. and Zhang et al. suggested a mechanism of two and four ORR pathway on N-doped graphene.⁴¹⁻⁴² Recently, N-doped graphene reached over 20% the diffusion-limited current density compared to Pt/C electrode.³² Shao et al. demonstrated high stability nitrogen-doped during ORR compared with the commercial Pt.³⁶ Furthermore, N-doped graphene can be used as photocatalysts,⁴³ ultra capacitors²⁹, etc.

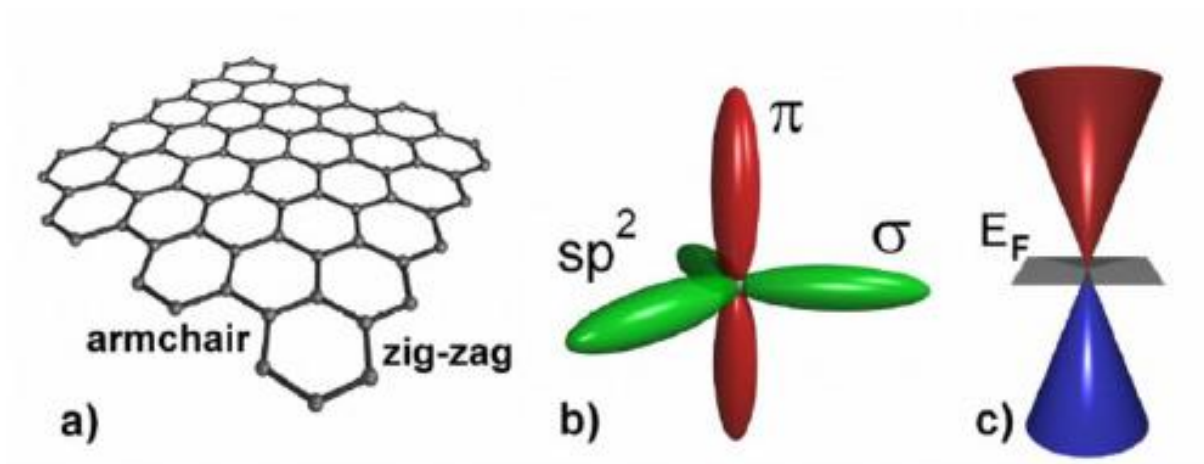


Figure 1. (a) Geometry of graphene. (b) Bonding of one carbon atom in graphene. (c) Band diagram of graphene at $K = 0$ point.¹

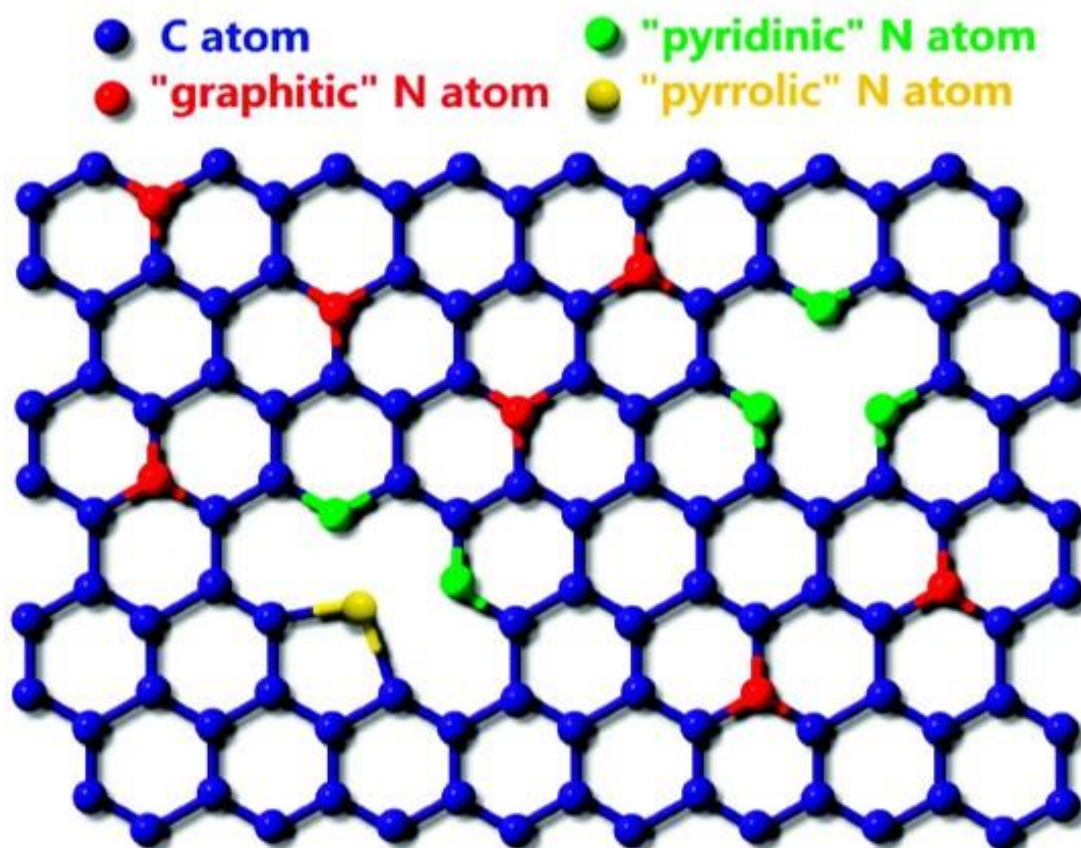


Figure 2. Schematic of N-doped graphene.



Figure 3. Examples of graphene application in various area.²

2. Conversion of polyacrylonitrile to N-doped graphene

As an acrylic fiber, polyacrylonitrile (PAN), is used as a precursor of carbon fibers (Figure 4a). Generally, PAN is made from acrylonitrile polymerization. It is relatively insoluble and hard as a semi-crystalline organic polymer. Many scientists have reported on the heat treatment of PAN because carbon fibers made from PAN have better properties than carbon fibers made from other precursors.⁴⁴⁻⁴⁶ In addition, when PAN is converted to carbon fibers, it exhibits a high carbon yield, which means that it is an appropriate precursor for mass production. The process of converting PAN to carbon fiber is divided into three stages: stabilization, carbonization, and graphitization.⁴⁷ The stabilization process is important for forming high-quality carbon materials (figure 4b). The process commonly proceeds in air because of oxygen. Oxygen leads to dehydrogenation of PAN and crosslink between PAN polymers.⁴⁸ During the process, cyclization and dehydrogenation reactions occur at the same time, and dehydrogenation occurs when oxygen is combined with hydrogen in PAN to form water. The PAN structure changes from a linear structure to an aromatic structure during the cyclization process, where the $C \equiv N$ bond, which is composed of PAN, is changed to $C = N$ bond.⁴⁹ Setnescu et al. reported PAN formed $C = C$ and $C = H$ during cyclization.⁵⁰ From their result, PAN forms highly stable aromatic structures. Generally, the temperature required for stabilization is approximately 180°C to 300°C. If the temperature is below 180°C, stabilization is not completed. Additionally, stabilization at high temperatures can result in the burning of PAN. The carbonization process produces stabilized PAN aromatic growth and polymerization (figure 4c). The temperature required for carbonization is known to be approximately 600°C to 1300°C. During carbonization, H, N and O atoms are eliminated as gases.⁵¹ The heating rate of carbonization process is under 5°C/min because of danger of shrinkage. The graphitization process occurs up to 2000°C, and this process enhances the stiffness of fibers and orientation of basal planes.

2.1 Experimental section

2.1.1 Conversion of polyacrylonitrile to N-doped graphene using CVD

PAN (Sigma-Aldrich, M_w 150,000) was dissolved in DMF at a concentration of 0.25%. PAN solution was sonicated for 3 hours. Pt foil was cleaned in acetone for 5 min using sonicator. Pt foil was treated O_2 plasma for 10 min to make the surface hydrophilic and to remove carbon residue. PAN solution was spin-coated on Pt foil at 3000 rpm for 2 min. The PAN film on Pt foil was loaded in a CVD system then heated at 200°C for 1 h under 2.0^{-1} torr. This process is essential for stabilization of PAN. The sample was heated to 900°C for 2 h under low pressure and then H_2 gas was introduced in chamber at 13 scem

for 30 min while maintaining the temperature for 1 h. The sample was cooled down approximately 3°C/min without any gas.

2.1.2 Transfer method

The N-doped graphene transferred onto SiO₂(300 nm)/Si substrate using the electrochemical bubbling method. For cleaning, SiO₂(300 nm)/Si substrate was sonicated in acetone solution for 5 min and in isopropyl alcohol solution for 5 min. PMMA was spin-coated on Graphene/Pt foil at 3000 rpm for 1 min. After that the sample was dried 70°C on the hot plate. The sample was used as the cathode, and pure Pt foil was used as the anode. The electrolyte used a NaOH aqueous solution (1.0 M). Current and voltage condition were 1 V and 0.8 A. When PMMA/graphene was peeled off from Pt foil, the sample was cleaned 2 times using deionized water to remove NaOH. Cleaned sample was transferred onto SiO₂(300 nm)/Si substrate. After that, the sample was dried in air and then immersed into acetone solution for removing PMMA.

2.1.3 FET fabrication

The N-doped graphene was transferred to on SiO₂(300 nm)/Si substrate. Oxygen-plasma treatment was performed to make graphene channel. E-beam lithography was used to fabricate source and drain. Au (55 nm)/(Ti 5nm) were deposited on the sample for forming source and drain by E-beam evaporator. After that, lift off method was employed to make pattern electrodes. The fabricated sample was heated at 300°C for 1 h to obtain good contact and remove polymer residue.

2.1.4 Characterization

The Raman spectroscopy was performed on alpha 300R Raman spectrometer (WITec) equipped with a 532 nm laser. The surface morphologies were characterized by scanning micro scope (S-4800, Hitachi). The atomic force microscope image was obtained by a DI-3100 AFM microscopy (Veeco) with tapping mode. The chemical composition of samples was studied by X-ray photoelectron spectra (K-Alpha, Thermo Fisher). The electrical properties of the samples were characterized by four tip probe station (4200-SCS, KEITHLEY).

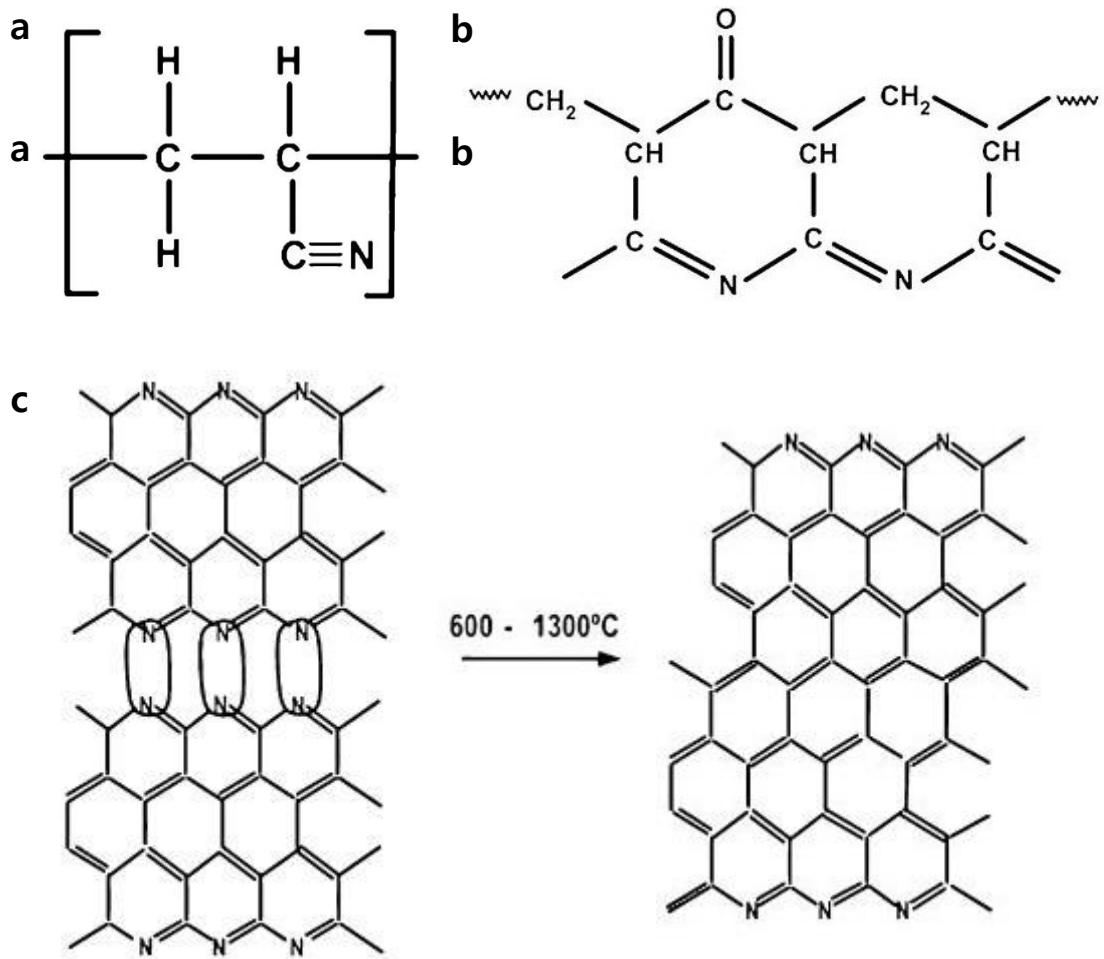


Figure 4. (a) Molecular structure of PAN. (b) The stabilized PAN structure.³ (c) Structure changes for PAN precursor during carbonization.⁴

2.2 Result and discussion

Figure 5a shows our experiment condition for conversion N-doped graphene using PAN. To stabilize PAN, the sample was spin-coated on Pt foil and heated at 200°C for 1 h under atmospheric pressure. To identify stabilization of PAN, the PAN and stabilized PAN that was heated at 200°C for 1 h under atmospheric pressure were examined with XPS to characterize any change in chemical structures. Figure 5b exhibits the C1s core-level spectra of PAN. The C1s peak could be fitted into three peaks at 284.7, 285.6 and 286.3 eV. The left peak at 286.3 eV is identified as the C \equiv N groups. The middle peak at 285.6 eV is attributed to CH-CN groups. The right peak at 284.7 eV correspond to CH₂ groups. The ratio of each peak areas is similar. that means C \equiv N : CH-CN : CH₂ is approximately equal to the expected rate of PAN values. That results are similar to results reported previously.⁵² Figure 5c exhibits the C1s core-level spectra of stabilized PAN. For stabilized PAN, the C1s spectrum could be fitted into six peaks. These peaks were assigned to sp²-C (284.0 eV), sp³-C (284.8 eV), CH-CN (285.6 eV), C = N and C \equiv N (286.3 eV), C-O and C-N (287.4 eV) and C = O (288.8 eV). Compared with the XPS spectrum of PAN, the intensities of CH₂, CH-CN and C = N, C \equiv N peaks are smaller than the XPS spectrum of PAN. Moreover, the peak at 284.0 eV for the sp²-C group and the peak at 287.4 eV for the C-N group, which was not observed as PAN, appeared after the stabilization process. These results indicate that most of the carbon were converted to aromatic rings, and the structure of PAN changed to stabilized PAN. Owing to the oxidation of PAN, the peak at 288.8 eV, corresponding to C = O appears in the XPS spectra of the stabilized PAN.

To confirm the stabilization effect, we performed two comparative experiments. The first experiment is N-doped graphene growth without the stabilization process. Figure 6a shows the SEM image of N-doped graphene morphology without the stabilization process. The SEM image shows that the graphene has many holes and the substrate is not completely covered with the film. This is because the stabilized PAN has only 33% of weight loss when heated to 700° C. However, at the same conditions, the weight loss of PAN is approximately 60%.⁵³ Hence, the formation of graphene was not perfect because of volatilization of PAN. The second experiment is N-doped graphene growth at vacuum during the stabilization process. Figure 6b shows The SEM image of graphene growth at vacuum during the stabilization process. The morphology of graphene is small and not forming continuous film. Because a PAN back-bone containing oxygen bearing groups provides better stability to sustain during carbonization treatment.⁴⁸

Figure 7 shows surface the morphology of our N-doped graphene. To investigate surface morphology, the N-doped graphene was transferred on 300-nm-thick SiO₂/Si substrates. as shown in figure 7a. A continuous and large-area film of N-doped graphene was observed via the optical image. Figure 7b shows the SEM image of N-doped graphene. The layers of graphene can be checked, in contrast to SEM image. The SEM image shows that a continuous graphene with some adlayer. That may be due to the

resorption of carbon. The AFM image shows that the thickness of the N-doped graphene is approximately 0.68 nm, suggesting that it consists of a single layer film (Figure 7c, 7d).

Raman spectroscopy is one of the most effective tools for identifying graphene (Figure 8). There are well known three Raman peaks for graphene. The D band, which is located at approximately 1344 cm^{-1} is associated with graphene defects. The D band does not appear to be pristine graphene. In the Raman spectra, the D band is one of the evidence that nitrogen is doped into graphene, because nitrogen causes vacancies and bonding disorder in graphene lattice. The G band is observed at approximately 1585 cm^{-1} in figure 8 pristine graphene. The G band occurs because of the E_{2g} phonon mode at the Γ point. The G band shift occurs because of many factors, such as doping, defects, strains and layer numbers. Moreover, our Raman spectra result is similar to the result obtained from previous data, where doping causes a blue shift in the G band.⁵⁴⁻⁵⁵ The Raman peak at approximately 2670 cm^{-1} is called the 2D band, which is a second-order zone boundary phonon mode to graphene. The 2D band shift occurs depending on the layer number, doping, and stacking. The intensity ratio of the G band and the 2D band (I_{2D}/I_G) and the 2D band of full width at half-maximum (FWHM) are applied to determine the graphene layers. The I_{2D}/I_G of N-doped graphene is 2.3. The FWHM of N-doped graphene is 40. The results indicate that our N-doped graphene is a single layer graphene. These results are consistent with the AFM and the SEM results.

To investigate the bonding configurations of N-doped graphene and N/C atomic ratio, the samples were examined with XPS. The N1s peak is observed in the typical XPS results of N-doped graphene (figure 9a). It is also clear that nitrogen is included in the sample compared to N-doped graphene and clean SiO₂ / Si substrates (inset of Figure 9c, 9c). Figure 9b shows the C 1s spectra of N-doped graphene. The C1s peak can be fitted with four components at 284.2 eV, 285.4 eV, 286.6 eV and 288.3 eV. The main peak, which is located at 284.2 eV, is assigned to graphite-like sp^2 carbon. The smallest peak, which is located at 288.3 eV, is CO type bond. It can be attributed to physisorbed oxygen on N-doped graphene or the incompleteness of deoxidation during the carbonization process. Two small peaks, which are located at 285.4 eV and 286.6 eV, correspond to N- sp^2 -C and N- sp^3 -C, respectively, which originate from the substitutional doping of nitrogen atoms.⁵⁴ The N1s peak in N-doped graphene is shown in figure 9c. The N1s peak can deconvolute three peaks at 398.5 eV, 399.4 eV and 400.3 eV. These peaks correspond to pyridinic-N, pyrrolic-N and graphitic-N. In our spectra, the intensities of pyridinic-N and pyrrolic-N are bigger than the intensity of graphitic-N. The result is consistent with previous theoretical prediction, which is that nitrogen atoms are more stable at the edges of graphene lattice than at the centers of graphene lattice.¹⁶ Figure 9d shows the changes in the ratio of carbon to nitrogen with the conversion temperature. Because the main reaction is the stabilization process up to 200°C, the ratio of nitrogen atoms is not significantly reduced. However, the rate of nitrogen atoms decreases rapidly from 800°C because nitrogen atoms were eliminated during the carbonization process.⁴⁷ As the temperature

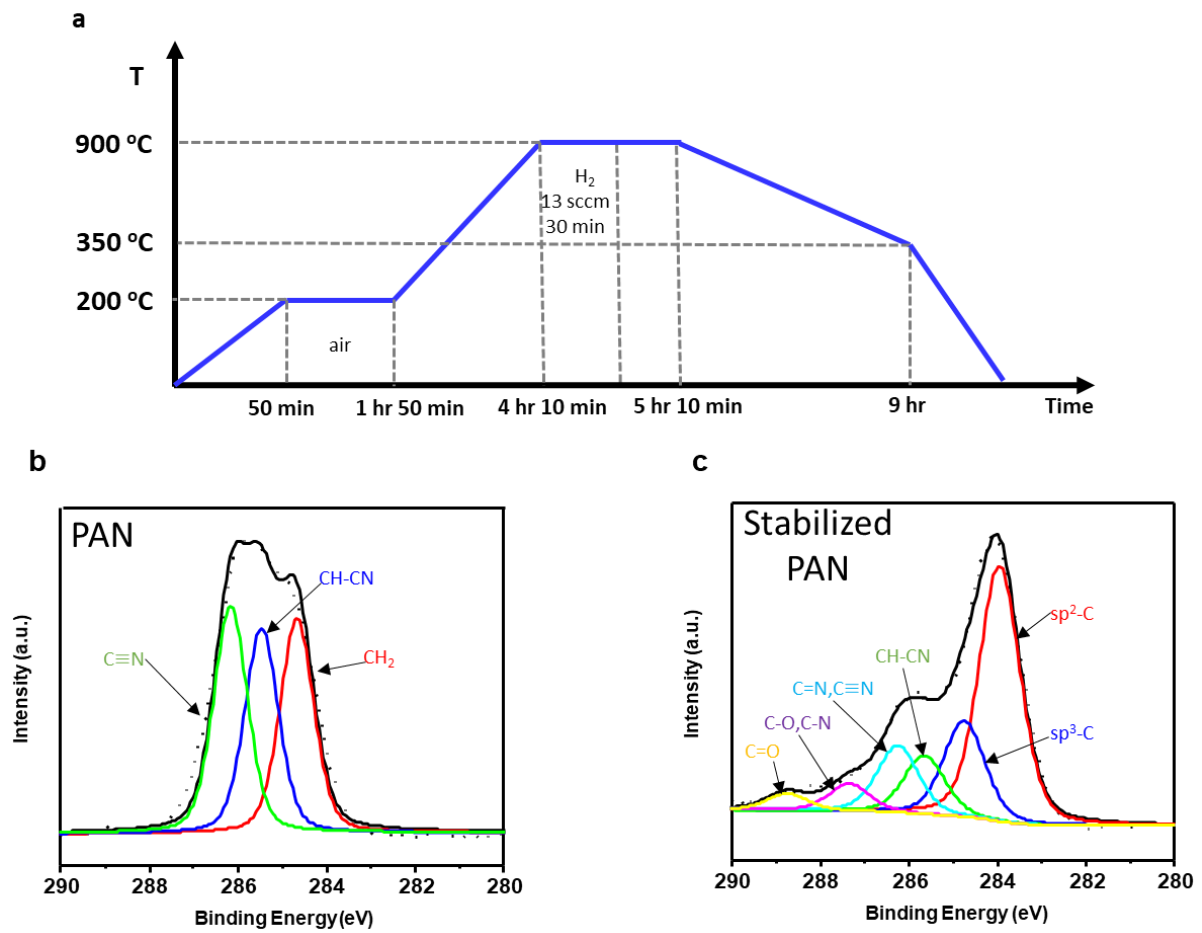


Figure 5. (a) Experiment process of conversion of PAN to N-doped graphene using CVD. (b) XPS C 1s spectrum of the PAN. (c) XPS C 1s spectrum of the stabilized PAN.

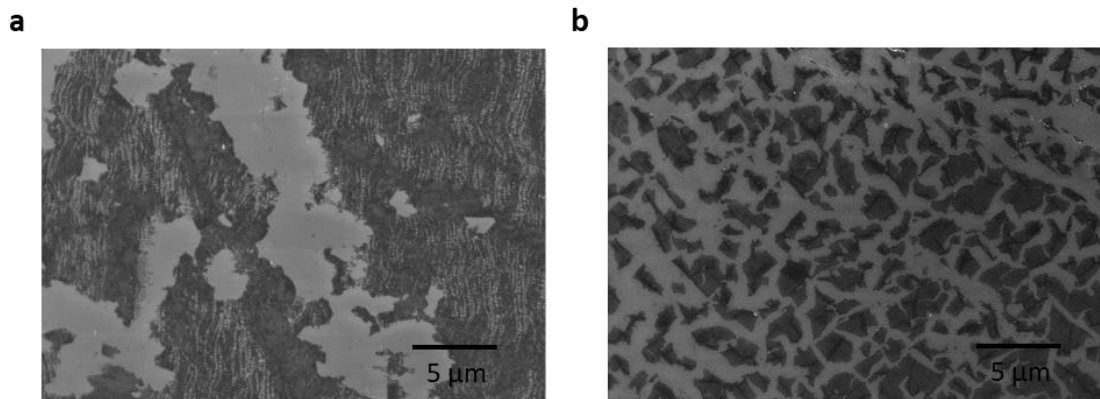


Figure 6. (a) SEM image of the N-doped graphene without stabilization process. (b) SEM image of the N-doped graphene growth at vacuum during the stabilization process.

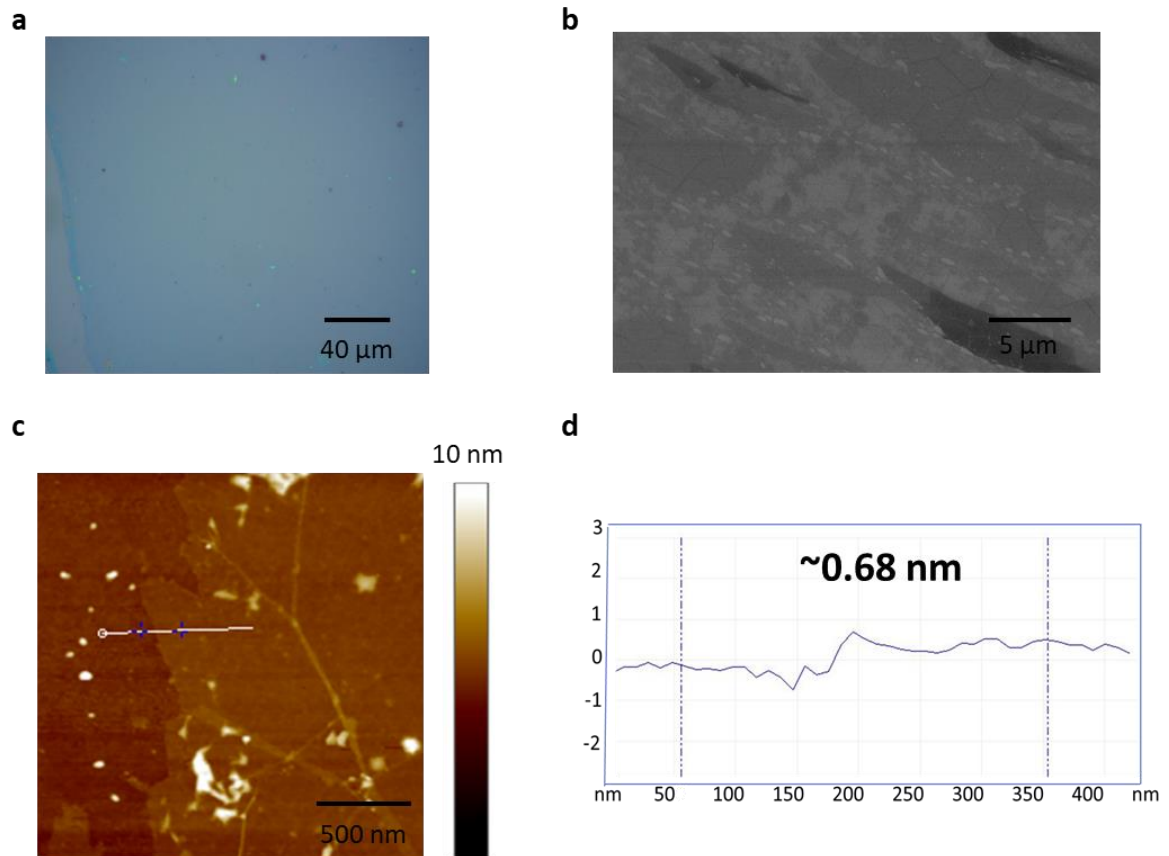


Figure 7. (a) Optic image of the N-doped graphene. (b) SEM image of the N-doped graphene. (c) AFM image of the N-doped graphene. (d) The height profile which was taken from (c) the white line.

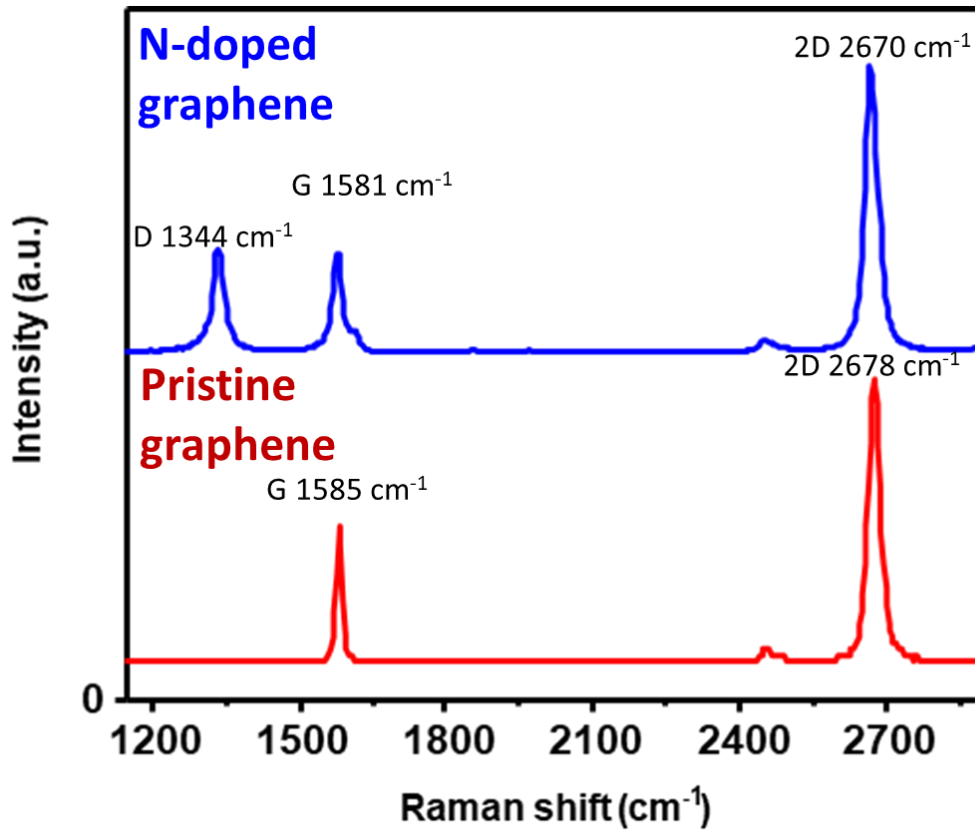


Figure 8. Raman spectra of the N-doped graphene, the spectrum of red line is pristine graphene. The spectrum of the blue line is the N-doped graphene.

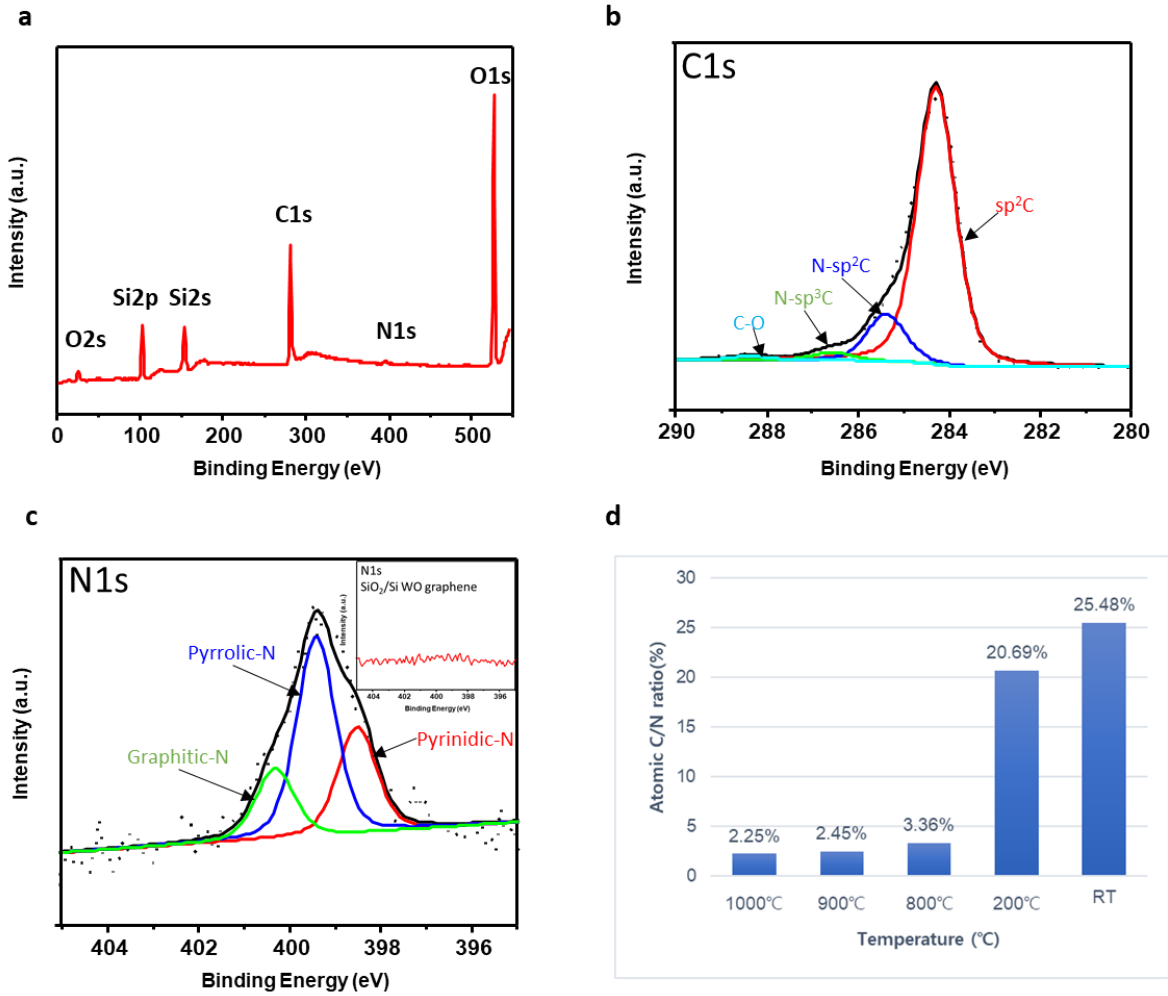


Figure 9. (a) XPS spectrum of the N-doped graphene on SiO₂(300 nm)/Si substrate. (b) XPS C 1s spectrum and (c) XPS N1s spectrum of the N-doped graphene on SiO₂(300 nm)/Si substrate. The inset image exhibits XPS N1s spectrum of cleaned SiO₂/Si substrate. (d) Graph of Atomic N ratio.

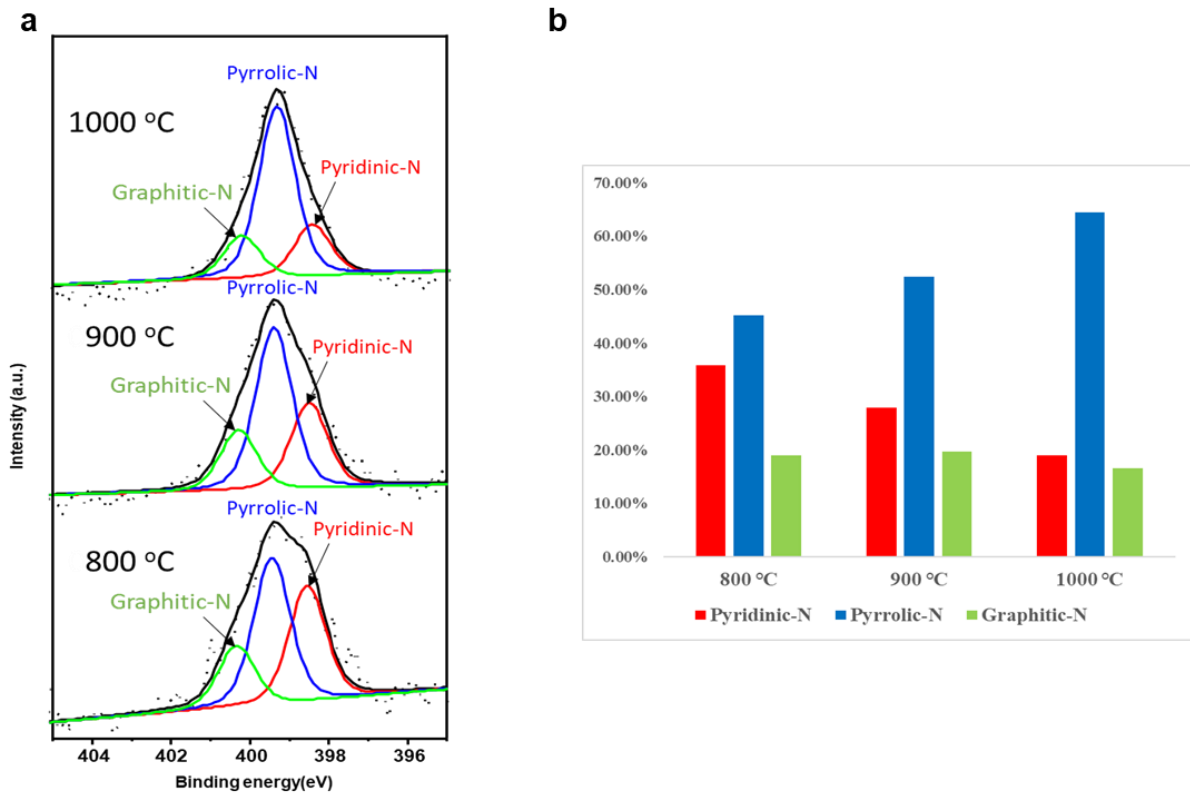


Figure 10. (a) XPS N 1s spectra of N-doped graphene with temperature. (b) Graph of N-doped graphene nitrogen configuration with temperature.

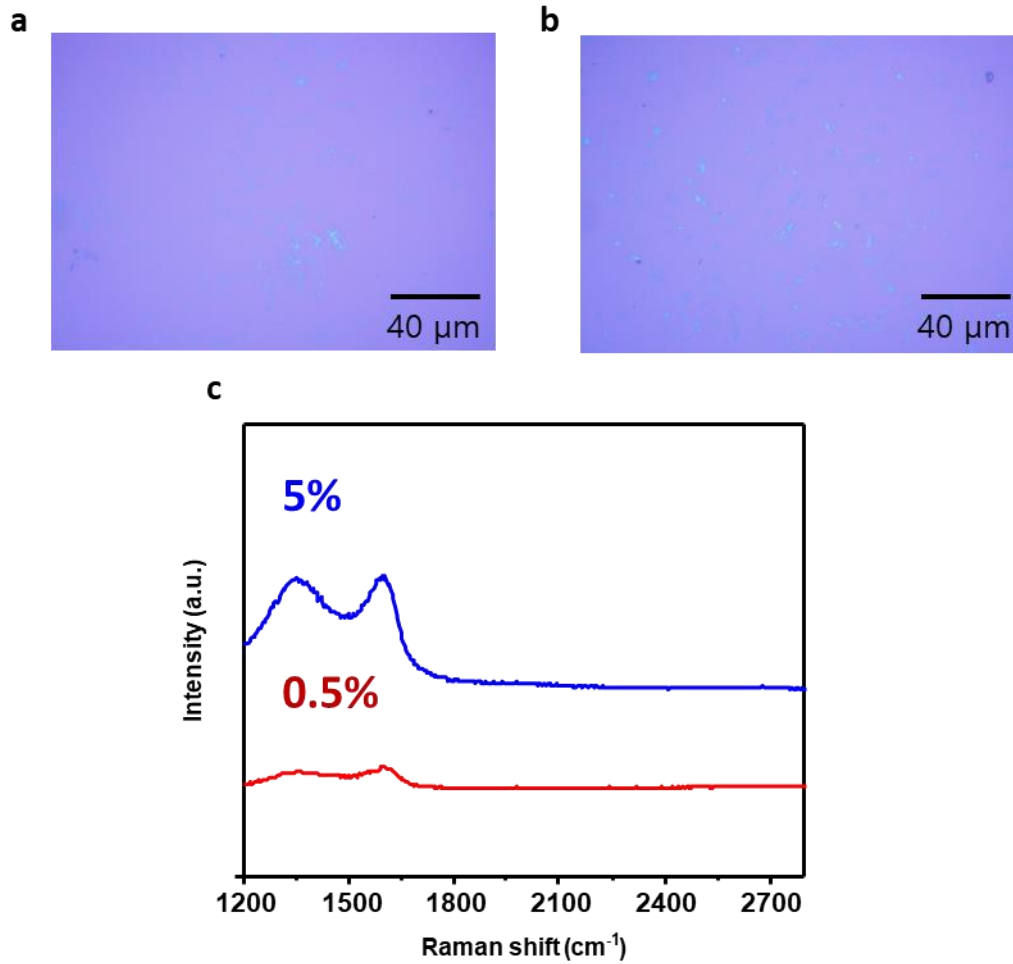


Figure 11. Optic image of different concentrations of PAN after the same conversion condition not using Pt but using Cu. (a) and (b) were used 0.5 and 5% PAN solution. (c). Raman spectra of PAN after the same conversion condition using Cu. Red and blue line were used 0.5 and 5% PAN solution.

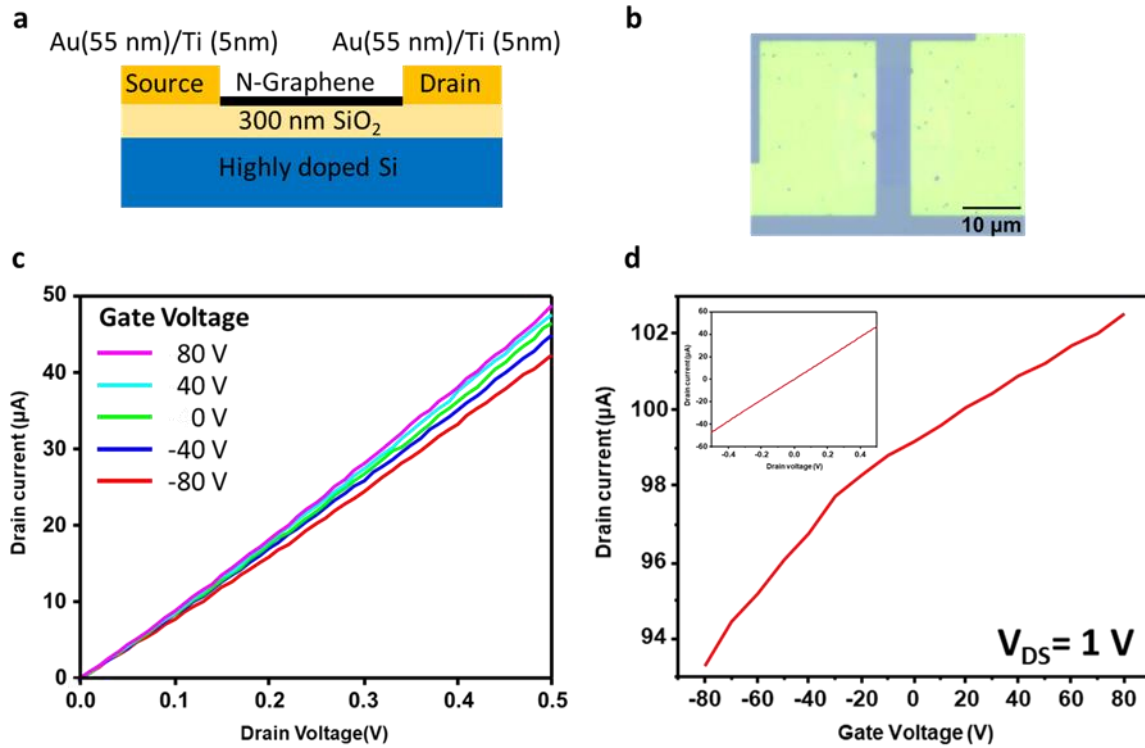


Figure 12. (a) Schematic of the N-doped graphene FET device. (b) Optic image of the N-doped graphene device. (c) I_{ds}/V_{ds} characteristics at various V_g for the N-doped graphene FET. Devices. (d) I_{ds}/V_g curve of the N-doped graphene ($V_{ds}=1$ V). The inset figure shows I_{ds}/V_{ds} characters without V_g .

increases from 800°C to 1000°C, the rate of nitrogen atoms decreases smoothly. Figure 10a shows XPS N 1-s spectra of N-doped graphene with temperature. As the conversion temperature increases, the ratio of pyridinic-N reduces. The denitrogenation occurs at the pyridinic N sites during the generation of HCN and NH₃.⁴⁷ The ratio of pyrrolic-N and the temperature are proportional to each other, which is similar to the relationship obtained in previous report.⁵⁶⁻⁵⁷

To investigate whether other graphene catalysts could convert PAN to N-doped graphene under our condition, we tried converting PAN to N-doped graphene using copper with the same experimental process. Figure 11a and b show optic images of the sample transferred on SiO₂/Si substrate. Although using 5% PAN solution shows much more carbon residues than 0.5% PAN solution, both images show many vacancies and small carbon residues. The appearance of carbon residues in both images appears to be a cluster of polymers rather than graphene. As shown in figure 11c, 2D peak was not observed in both samples. That means copper and Pt have different converting mechanisms of PAN to N-doped graphene. The reasons for not successfully converting PAN to N-doped graphene may be due to oxygen in polymers as air changes copper to copper oxide, which has a rare catalytic effect to form graphene, or because copper has a weaker graphitization ability compared to Pt.⁵⁸⁻⁵⁹

We fabricated the bottom gated field-effect transistors (FETs) of N-doped graphene to identify electrical characteristics of nitrogen doping effects. As shown in figure 12a, N-doped graphene acts as conducting channel of FETs. Figure 12b shows optic image of FETs. The channel length was 6.5 μm and the channel width was 20.3 μm. The inset of figure 12d shows the source-drain current (I_{ds}) vs the source drain voltage (V_{ds}) behavior without back-gate voltage. The result indicates ohmic contact forming between the N-doped graphene and the Au/Ti pads, which acts as a source and drain. Figure 12c shows the I_{ds} vs V_{ds} behavior at variable back-gate voltages (V_g) from -80 V to 80 V in a step of 40 V. The figure shows that the I_{ds} decreases as the V_g decreases, which is consistent with n-type behavior. Figure 12d shows the I_{ds} dependence on V_g behavior for the N-doped graphene at a fixed V_{ds} of 1.0 V. The drain current increases as the gate voltage increases, indicating the channel is n-type. Dirac points were not observed because of limitations in our equipment. The electron mobility is estimated by the equation.⁶⁰

$$\mu = \frac{\Delta I_{ds}}{\Delta V_{gs}} * \frac{L}{WC_{ox}V_{ds}} \quad (1)$$

where L and W denote channel length and channel width, respectively, and C_{ox} is the capacitance per unit area of the gate insulator, which is SiO₂(300 nm) in the sample. The N-doped graphene mobility is approximately 4.7 cm²V⁻¹s⁻¹ according to equation (1). This value is similar to the value obtained in

previous reports^{18, 61-62}. However, the mobility is approximately two orders of magnitude reduced compared to pristine graphene devices.⁶¹ That may be due to pyridinic and substituting nitrogen in graphene lattice induces more scattering in graphene lattice. Additionally, oxygen residue or physisorption can be one of the reasons.

2.3 Conclusion

In conclusion, we report a method that converts polyacrylonitrile to N-doped graphene films. During the process, stabilization becomes an important factor because of dehydrogenation and cyclization reaction. The converted N-doped graphene exhibits a continuous film with a monolayer. The nitrogen substitution site of graphene was pyrrolic-N site. The fabricated FET shows an n-type behavior, which is in accordance with XPS result. Electron mobility of the N-doped graphene is approximately $4.7 \text{ cm}^2 \text{V}^{-1} \text{s}^{-1}$. Nevertheless, improvement to quality is required to put to industrial use. PAN conversion to N-doped graphene has the potential to open the way to graphene commercialization.

REFERENCES

1. Lemme, M. C., Current Status of Graphene Transistors. *Solid state Phenomena* **2010**, *156-158*, 499-509.
2. Roddaro, S.; Pingue, P.; Piazza, V.; Pellegrini, V.; Beltram, F., The Optical Visibility of Graphene: Interference Colors of Ultrathin Graphite on SiO₂. *Nano Letters* **2007**, *7* (9), 2707-2710.
3. David LIB, I. A., Influence of the thermostabilization process and soak time during pyrolysis process on the polyacrylonitrile carbon membranes for O₂/N₂ separation. *Journal of Membrane Science* **2002**, *213* (1-2), 285-291.
4. Zhu, D.; Xu, C. Y.; Nakura, N.; Matsuo, M., Study of carbon films from PAN/VGCF composites by gelation/crystallization from solution. *Carbon* **2002**, *40* (3), 363-373.
5. Novoselov, K. S.; Geim, A. K.; Morozov, S. V.; Jiang, D.; Zhang, Y.; Dubonos, S. V.; Grigorieva, I. V.; Firsov, A. A., Electric field effect in atomically thin carbon films. *Science* **2004**, *306* (5696), 666-669.
6. Mayorov, A. S.; Gorbachev, R. V.; Morozov, S. V.; Britnell, L.; Jalil, R.; Ponomarenko, L. A.; Blake, P.; Novoselov, K. S.; Watanabe, K.; Taniguchi, T.; Geim, A. K., Micrometer-Scale Ballistic Transport in Encapsulated Graphene at Room Temperature. *Nano Letters* **2011**, *11* (6), 2396-2399.
7. Geim, A. K.; Novoselov, K. S., The rise of graphene. *Nat Mater* **2007**, *6* (3), 183-91.
8. Lee, C.; Wei, X.; Kysar, J. W.; Hone, J., Measurement of the Elastic Properties and Intrinsic Strength of Monolayer Graphene. *Science* **2008**, *321* (5887), 385-388.
9. Lee, J. U.; Yoon, D.; Cheong, H., Estimation of Young's Modulus of Graphene by Raman Spectroscopy. *Nano Letters* **2012**, *12* (9), 4444-4448.
10. Nair, R. R.; Blake, P.; Grigorenko, A. N.; Novoselov, K. S.; Booth, T. J.; Stauber, T.; Peres, N. M. R.; Geim, A. K., Fine Structure Constant Defines Visual Transparency of Graphene. *Science* **2008**, *320* (5881), 1308-1308.
11. Ni, Z. H.; Wang, H. M.; Kasim, J.; Fan, H. M.; Yu, T.; Wu, Y. H.; Feng, Y. P.; Shen, Z. X., Graphene thickness determination using reflection and contrast spectroscopy. *Nano Letters* **2007**, *7* (9), 2758-2763.
12. Blake, P.; Hill, E. W.; Neto, A. H. C.; Novoselov, K. S.; Jiang, D.; Yang, R.; Booth, T. J.; Geim, A. K., Making graphene visible. *Applied Physics Letters* **2007**, *91* (6), 063124.
13. Palik, E. D., *Handbook of optical constants of solids*. Academic Press: Orlando, 1985; p xviii, 804 p.
14. Ewels, C. P.; Glerup, M., Nitrogen doping in carbon nanotubes. *J Nanosci Nanotechno* **2005**, *5* (9), 1345-1363.
15. Wang, H. B.; Maiyalagan, T.; Wang, X., Review on Recent Progress in Nitrogen-Doped Graphene: Synthesis, Characterization, and Its Potential Applications. *Acs Catal* **2012**, *2* (5), 781-794.
16. Wang, X. R.; Li, X. L.; Zhang, L.; Yoon, Y.; Weber, P. K.; Wang, H. L.; Guo, J.; Dai, H. J., N-Doping of Graphene Through Electrothermal Reactions with Ammonia. *Science* **2009**, *324* (5928), 768-771.
17. Li, X.; Cai, W.; An, J.; Kim, S.; Nah, J.; Yang, D.; Piner, R.; Velamakanni, A.; Jung, I.; Tutuc, E.;

- Banerjee, S. K.; Colombo, L.; Ruoff, R. S., Large-Area Synthesis of High-Quality and Uniform Graphene Films on Copper Foils. *Science* **2009**, *324* (5932), 1312-1314.
18. Sun, Z.; Yan, Z.; Yao, J.; Beitler, E.; Zhu, Y.; Tour, J. M., Growth of graphene from solid carbon sources. *Nature* **2010**, *468* (7323), 549-552.
 19. Hummers, W. S.; Offeman, R. E., Preparation of Graphitic Oxide. *Journal of the American Chemical Society* **1958**, *80* (6), 1339-1339.
 20. Berger, C.; Song, Z. M.; Li, T. B.; Li, X. B.; Ogbazghi, A. Y.; Feng, R.; Dai, Z. T.; Marchenkov, A. N.; Conrad, E. H.; First, P. N.; de Heer, W. A., Ultrathin epitaxial graphite: 2D electron gas properties and a route toward graphene-based nanoelectronics. *J Phys Chem B* **2004**, *108* (52), 19912-19916.
 21. Li, X.; Cai, W.; Colombo, L.; Ruoff, R. S., Evolution of Graphene Growth on Ni and Cu by Carbon Isotope Labeling. *Nano Letters* **2009**, *9* (12), 4268-4272.
 22. Sutter, P.; Sadowski, J. T.; Sutter, E., Graphene on Pt(111): Growth and substrate interaction. *Physical Review B* **2009**, *80* (24).
 23. Sutter, E.; Albrecht, P.; Sutter, P., Graphene growth on polycrystalline Ru thin films. *Applied Physics Letters* **2009**, *95* (13).
 24. Lee, J. H.; Lee, E. K.; Joo, W. J.; Jang, Y.; Kim, B. S.; Lim, J. Y.; Choi, S. H.; Ahn, S. J.; Ahn, J. R.; Park, M. H.; Yang, C. W.; Choi, B. L.; Hwang, S. W.; Whang, D., Wafer-Scale Growth of Single-Crystal Monolayer Graphene on Reusable Hydrogen-Terminated Germanium. *Science* **2014**, *344* (6181), 286-289.
 25. Yan, Z.; Peng, Z. W.; Sun, Z. Z.; Yao, J.; Zhu, Y.; Liu, Z.; Ajayan, P. M.; Tour, J. M., Growth of Bilayer Graphene on Insulating Substrates. *Acs Nano* **2011**, *5* (10), 8187-8192.
 26. Byun, S.-J.; Lim, H.; Shin, G.-Y.; Han, T.-H.; Oh, S. H.; Ahn, J.-H.; Choi, H. C.; Lee, T.-W., Graphenes Converted from Polymers. *J. Phys. Chem. Lett.* **2011**, *2* (5), 493-497.
 27. Hye JIN Jo, J. H. L., Rodeny S ruoff, Hyunseob Lim, Seong In Yoon, Hu Young Jeong, Tae Joo Shin, Christopher W Bielawski, Hyeon Suk Shin, Conversion of Langmuir-Blodgett monolayers and bilayers of poly(amic acid) through polyimide to graphene. *2D materials* **2017**, *4* (1), 014005.
 28. Lee, E.; Lee, H. C.; Jo, S. B.; Lee, H.; Lee, N.-S.; Park, C. G.; Lee, S. K.; Kim, H. H.; Bong, H.; Cho, K., Heterogeneous Solid Carbon Source-Assisted Growth of High-Quality Graphene via CVD at Low Temperatures. *Adv. Funct. Mater.* **2016**, *26* (4), 562-568.
 29. Wen, Z. H.; Wang, X. C.; Mao, S.; Bo, Z.; Kim, H.; Cui, S. M.; Lu, G. H.; Feng, X. L.; Chen, J. H., Crumpled Nitrogen-Doped Graphene Nanosheets with Ultrahigh Pore Volume for High-Performance Supercapacitor. *Advanced Materials* **2012**, *24* (41), 5610-5616.
 30. Palnitkar, U. A.; Kashid, R. V.; More, M. A.; Joag, D. S.; Panchakarla, L. S.; Rao, C. N. R., Remarkably low turn-on field emission in undoped, nitrogen-doped, and boron-doped graphene. *Applied Physics Letters* **2010**, *97* (6).
 31. Kashid, R. V.; Yusop, M. Z.; Takahashi, C.; Kalita, G.; Panchakarla, L. S.; Joag, D. S.; More, M. A.; Tanemura, M., Field emission characteristics of pristine and N-doped graphene measured by in-situ transmission electron microscopy. *Journal of Applied Physics* **2013**, *113* (21).
 32. Qu, L. T.; Liu, Y.; Baek, J. B.; Dai, L. M., Nitrogen-Doped Graphene as Efficient Metal-Free

Electrocatalyst for Oxygen Reduction in Fuel Cells. *Acs Nano* **2010**, *4* (3), 1321-1326.

33. Luo, Z. Q.; Lim, S. H.; Tian, Z. Q.; Shang, J. Z.; Lai, L. F.; MacDonald, B.; Fu, C.; Shen, Z. X.; Yu, T.; Lin, J. Y., Pyridinic N doped graphene: synthesis, electronic structure, and electrocatalytic property. *J Mater Chem* **2011**, *21* (22), 8038-8044.
34. Panchokarla, L. S.; Subrahmanyam, K. S.; Saha, S. K.; Govindaraj, A.; Krishnamurthy, H. R.; Waghmare, U. V.; Rao, C. N. R., Synthesis, Structure, and Properties of Boron- and Nitrogen-Doped Graphene. *Advanced Materials* **2009**, *21* (46), 4726-+.
35. Liu, Q.; Guo, B. D.; Rao, Z. Y.; Zhang, B. H.; Gong, J. R., Strong Two-Photon-Induced Fluorescence from Photostable, Biocompatible Nitrogen-Doped Graphene Quantum Dots for Cellular and Deep-Tissue Imaging. *Nano Letters* **2013**, *13* (6), 2436-2441.
36. Shao, Y. Y.; Zhang, S.; Engelhard, M. H.; Li, G. S.; Shao, G. C.; Wang, Y.; Liu, J.; Aksay, I. A.; Lin, Y. H., Nitrogen-doped graphene and its electrochemical applications. *J Mater Chem* **2010**, *20* (35), 7491-7496.
37. Jo, G.; Choe, M.; Lee, S.; Park, W.; Kahng, Y. H.; Lee, T., The application of graphene as electrodes in electrical and optical devices. *Nanotechnology* **2012**, *23* (11).
38. Maiyalagan, T.; Dong, X. C.; Chen, P.; Wang, X., Electrodeposited Pt on three-dimensional interconnected graphene as a free-standing electrode for fuel cell application. *J Mater Chem* **2012**, *22* (12), 5286-5290.
39. Wang, H. B.; Zhang, C. J.; Liu, Z. H.; Wang, L.; Han, P. X.; Xu, H. X.; Zhang, K. J.; Dong, S. M.; Yao, J. H.; Cui, G. L., Nitrogen-doped graphene nanosheets with excellent lithium storage properties. *J Mater Chem* **2011**, *21* (14), 5430-5434.
40. Reddy, A. L. M.; Srivastava, A.; Gowda, S. R.; Gullapalli, H.; Dubey, M.; Ajayan, P. M., Synthesis Of Nitrogen-Doped Graphene Films For Lithium Battery Application. *Acs Nano* **2010**, *4* (11), 6337-6342.
41. Zhang, L. P.; Xia, Z. H., Mechanisms of Oxygen Reduction Reaction on Nitrogen-Doped Graphene for Fuel Cells. *J Phys Chem C* **2011**, *115* (22), 11170-11176.
42. Kurak, K. A.; Anderson, A. B., Nitrogen-Treated Graphite and Oxygen Electroreduction on Pyridinic Edge Sites. *J Phys Chem C* **2009**, *113* (16), 6730-6734.
43. Han, B.; Liu, S. Q.; Tang, Z. R.; Xu, Y. J., Electrostatic self-assembly of CdS nanowires-nitrogen doped graphene nanocomposites for enhanced visible light photocatalysis. *J Energy Chem* **2015**, *24* (2), 145-156.
44. Xiao, H.; Lu, Y. G.; Zhao, W. Z.; Qin, X. Y., The effect of heat treatment temperature and time on the microstructure and mechanical properties of PAN-based carbon fibers. *J Mater Sci* **2014**, *49* (2), 794-804.
45. Guigon, M.; Oberlin, A., Heat-Treatment of High-Tensile Strength Pan-Based Carbon-Fibers - Microtexture, Structure and Mechanical-Properties. *Compos Sci Technol* **1986**, *27* (1), 1-23.
46. Kaburagi, Y.; Hishiyama, Y., Highly crystallized graphite films prepared by high-temperature heat treatment from carbonized aromatic polyimide films. *Carbon* **1995**, *33* (6), 773-777.
47. Rahaman, M. S. A.; Ismail, A. F.; Mustafa, A., A review of heat treatment on polyacrylonitrile

fiber. *Polymer Degradation and Stability* **2007**, *92* (8), 1421-1432.

48. Rangarajan, P.; Bhanu, V. A.; Godshall, D.; Wilkes, G. L.; McGrath, J. E.; Baird, D. G., Dynamic oscillatory shear properties of potentially melt processable high acrylonitrile terpolymers. *Polymer* **2002**, *43* (9), 2699-2709.

49. Fitzer, E.; Muller, D. J., Influence of Oxygen on Chemical-Reactions during Stabilization of Pan as Carbon-Fiber Precursor. *Carbon* **1975**, *13* (1), 63-69.

50. Setnescu, R.; Jipa, S.; Setnescu, T.; Kappel, W.; Kobayashi, S.; Osawa, Z., IR and X-ray characterization of the ferromagnetic phase of pyrolysed polyacrylonitrile. *Carbon* **1999**, *37* (1), 1-6.

51. Wang, S.; Chen, Z. H.; Ma, W. J.; Ma, Q. S., Influence of heat treatment on physical-chemical properties of PAN-based carbon fiber. *Ceram Int* **2006**, *32* (3), 291-295.

52. Li, L.; Chan, C. M.; Weng, L. T., Effects of the sequence distribution of poly(acrylonitrile-butadiene) copolymers on the surface chemical composition as determined by XPS and dynamic contact angle measurements. *Macromolecules* **1997**, *30* (12), 3698-3700.

53. Sunho Lee, J. K., Bon-Cheol Ku, Junkyung Kim, Han-Ik Joh, Structural Evolution of Polyacrylonitrile Fibers in Stabilization and Carbonization. *Advances in Chemical Engineering and Science* **2012**, *2*, 275-282.

54. Wei, D. C.; Liu, Y. Q.; Wang, Y.; Zhang, H. L.; Huang, L. P.; Yu, G., Synthesis of N-Doped Graphene by Chemical Vapor Deposition and Its Electrical Properties. *Nano Letters* **2009**, *9* (5), 1752-1758.

55. Yang, Q. H.; Hou, P. X.; Unno, M.; Yamauchi, S.; Saito, R.; Kyotani, T., Dual Raman features of double coaxial carbon nanotubes with N-doped and B-doped multiwalls. *Nano Letters* **2005**, *5* (12), 2465-2469.

56. Pels, J. R.; Kapteijn, F.; Moulijn, J. A.; Zhu, Q.; Thomas, K. M., Evolution of Nitrogen Functionalities in Carbonaceous Materials during Pyrolysis. *Carbon* **1995**, *33* (11), 1641-1653.

57. Lai, L. F.; Potts, J. R.; Zhan, D.; Wang, L.; Poh, C. K.; Tang, C. H.; Gong, H.; Shen, Z. X.; Jianyi, L. Y.; Ruoff, R. S., Exploration of the active center structure of nitrogen-doped graphene-based catalysts for oxygen reduction reaction. *Energ Environ Sci* **2012**, *5* (7), 7936-7942.

58. Hao, Y. F.; Bharathi, M. S.; Wang, L.; Liu, Y. Y.; Chen, H.; Nie, S.; Wang, X. H.; Chou, H.; Tan, C.; Fallahzad, B.; Ramanarayan, H.; Magnuson, C. W.; Tutuc, E.; Yakobson, B. I.; McCarty, K. F.; Zhang, Y. W.; Kim, P.; Hone, J.; Colombo, L.; Ruoff, R. S., The Role of Surface Oxygen in the Growth of Large Single-Crystal Graphene on Copper. *Science* **2013**, *342* (6159), 720-723.

59. Sun, J.; Nam, Y.; Lindvall, N.; Cole, M. T.; Teo, K. B. K.; Park, Y. W.; Yurgens, A., Growth mechanism of graphene on platinum: Surface catalysis and carbon segregation. *Applied Physics Letters* **2014**, *104* (15).

60. Parvez, K.; Li, R. J.; Puniredd, S. R.; Hernandez, Y.; Hinkel, F.; Wang, S. H.; Feng, X. L.; Mullen, K., Electrochemically Exfoliated Graphene as Solution-Processable, Highly Conductive Electrodes for Organic Electronics. *Acs Nano* **2013**, *7* (4), 3598-3606.

61. Jin, Z.; Yao, J.; Kittrell, C.; Tour, J. M., Large-Scale Growth and Characterizations of Nitrogen-

Doped Monolayer Graphene Sheets. *Acs Nano* **2011**, *5* (5), 4112-4117.

62. Li, X. Y.; Tang, T.; Li, M.; He, X. C., Nitrogen-doped graphene films from simple photochemical doping for n-type field-effect transistors. *Applied Physics Letters* **2015**, *106* (1).